

RESEARCH

Open Access



Adipocyte-derived CXCL10 in obesity promotes the migration and invasion of ovarian cancer cells

Zhe Wang^{1†}, Qingjian Ou^{2†}, Ying Liu³, Yuanyuan Liu¹, Qingwei Zhu¹, Jingqiu Feng¹, Fengze Han¹ and Lu Gao^{1,4*}

Abstract

Background As a widespread epidemic, obesity poses a significant risk to health and leads to physiological abnormalities, including diabetes mellitus and inflammation. Obesity-induced inflammation can accelerate the development of various cancers; however, the role of obesity in the migration of ovarian carcinoma is still unclear.

Results Twenty-four commonly upregulated genes were identified from single-cell RNA sequencing datasets of both ovarian carcinoma and adipose tissue of obese humans, with the chemokine CXCL10 showing a significant increase in adipose tissues associated with obesity. And CXCL10 treated primed macrophages exhibit both direct and indirect effects on the proliferation, apoptosis, migration, and invasion of ovarian adenocarcinoma cells. The treatment of CXCL10 on the SKOV3 cells enhances FAK expression and phosphorylation, thereby accelerating the migration and invasion of ovarian cancer cells. Conditioned medium-derived from CXCL10-treated THP-1 cells significantly promoted ovarian cancer cell migration and invasion, which may be attributed to the increased expression of C1QA, C1QC, CCL24, and IL4R in macrophages.

Conclusions Obesity exacerbates the production of CXCL10 from adipose tissues in obese women. CXCL10 is a key hub factor between developments of ovarian cancer and adipose tissues in obese. Targeting adipose-derived CXCL10 or its downstream macrophages may be a potential strategy to alleviate ovarian cancer accompanied by obesity.

Keywords CXCL10, Ovarian carcinoma, Obesity, Adipose tissue, Macrophage

Introduction

Obesity with excessive fat accumulation presents a risk to health and increases incidence of obesity-related complications. Excess nutrient intake can result in the expansion of adipose tissue to store energy and augmented adipose tissue induced inflammation, which is one of the features of obesity [1]. Adipose tissue in obesity can enhance the production of proinflammatory cytokines (such as IL-1, IL-6, and TNF) and chemokines from adipocytes and immune cells [2]. The chemokines, including CXCL1, CXCL5, CXCL10, and CXCL11, are upregulated in the adipose tissue of obesity [3, 4], and the expression of chemokine receptors, including CCR1, CCR2, CCR3, and CCR5, is also increased in the omental and subcutaneous adipose tissues of obesity [5, 6]. Moreover,

[†]Zhe Wang and Qingjian Ou contributed equally to this work and share first authorship.

*Correspondence:

Lu Gao
roadgao@163.com

¹ Department of Physiology, College of Basic Medical Sciences, Naval Medical University, Shanghai 200433, China

² Laboratory of Clinical and Visual Sciences, Tongji Hospital, School of Medicine, Tongji University, Shanghai 200331, China

³ School of Life Sciences, Bengbu Medical University, Anhui 233030, China

⁴ Shanghai Key Laboratory for Assisted Reproduction and Reproductive Genetics, Shanghai 200433, China



inflammation is thought to be linked to obesity, insulin resistance, metabolic syndrome, and even cancer [7, 8].

Several studies have demonstrated a positive correlation between obesity, as measured by BMI, and cancer incidence [9–12]. As the most fatal gynecologic cancer, ovarian cancer is an important source of cancer-related mortality worldwide. Most patients with ovarian cancer ultimately succumb to abdominal metastatic tumors rather than the primary carcinoma in situ [13]. The spread of ovarian cancer cells to abdominal tissues commonly occurs via peritoneal fluid [14]. Thus, the attachment between ovarian cancer cells and the omentum is the initial step for the further formation of peritoneal disease [15, 16]. Although the relationships between omentum metastasis and ovarian cancer were widely acknowledged, the role of obesity in the metastasis of ovarian carcinoma remains unclear.

Chemokines, classified into four subfamilies—CXC, CC, (X)C, and CX3C based on their structure—play a pivotal role in immune regulation and tumor development [17]. The chemokine itself can regulate tumor cell growth, invasiveness, metastasis, and angiogenesis [18–20]. Moreover, the chemokine can also recruit anti- or pro-tumor immune cells to the tumor microenvironment and affect tumor progression indirectly [21, 22]. For instance, CCL5 has been shown to recruit Treg cells to the tumor, facilitating tumor metastasis in ovarian cancer [20, 23]. CXCL10 and the receptor CXCR3 were overexpressed and associated with poor survival outcomes in pancreatic cancer [24, 25]. Obesity is characterized by the enormous production of proinflammatory cytokines and chemokines from adipocytes [26]. While epidemiologic studies revealed that the prognosis of ovarian cancer is significantly worse in obese women compared to those with a normal BMI [27–29]. Thus, it is of significant interest to investigate the roles and mechanisms of adipocyte-derived chemokines in the process of ovarian cancer, under the condition of obesity.

In this study, we integrated datasets of bulk RNA-sequencing or single cell RNA-sequencing in adipose tissues and ovarian cancer cells to discover common DEGs (differentially expressed genes) between obesity and ovarian cancer, and dissect the effects and underlying mechanisms of the chemokines produced by the adipose tissues on the biological characteristics of ovarian cancer cells. Our study may help identify a specific target for treating ovarian cancer occurred under the setting of obesity.

Materials and methods

Differentially expressed gene analysis in human and mice adipose tissues

The datasets of GSE152991 [30], GSE110729, and GSE132885 [31] were used to analyze the DEGs in white

adipose tissue between obese and normal mice based on the R package DESeq2 [32]. The differentially expressed genes (OB_DEG) were identified as a P -value < 0.05 and $\log_2FC > 1$ between obese and normal mice. For GSE152991, all samples in the groups of metabolically-healthy lean (MHL), metabolically-healthy obese (MHO), and metabolically-unhealthy obese (MUO) were included in the analyses, among which MHL was considered a control group [30]. For GSE110729, samples with a BMI of 20–23 were categorized as the control group, while samples with a BMI of 47–68 were classified as the obese group. For GSE132885, subcutaneous (or visceral) adipose tissues from C57BL/6 mice fed a standard chow diet (SCD) for 8 or 20 weeks were classified as the control groups, while tissues from mice fed a high-fat diet (HFD) were classified as the obese group.

Analysis of single-cell RNA sequencing data in white adipose between SCD and HFD mice

To illustrate the potential relationship between obesity and ovarian carcinoma at the single-cell level, we analyzed the datasets of GSE176171 [mouse (C57/B6)] inguinal white adipose from GSM5820692 (HFD), GSM5820693 (SCD), GSM5820694 (HFD), and GSM5820695 (SCD); mouse peri-ovarian white adipose from GSM5820698 (HFD), GSM5820699 (SCD), GSM5820700 (HFD), GSM5820701 (SCD)] following the typical pipeline of Seurat 4.4.0 [33]. Briefly, the matrix was normalized by the NormalizeData function, and the top 2000 highly variable genes were identified with the FindVariableGenes function. The tSNE and UMAP dimensionality reductions were used to project these populations in two dimensions, respectively. The cell types were annotated based on the published paper [34] and known markers [mesothelial cell: *Upk3b*; adipose stem and progenitor cell (ASPC): *Pdgfra*; adipocytes (APC): *Adipoq*; endometrial cell: *Prlr*; epithelial cell: *ErbB4*; endothelial cell: *Pecam1*; myeloid cell: *Mafb*; B cell: *Ms4a1*; T cells: *Il7r*; smooth muscle cell: *Acta2*]. The FeaturePlot function in R package Seurat (v4.4.0) and the function DotPlot in R package ggplot2 (v3.4.4) were used to visualize the gene expression.

Differentially expressed gene analyses between ovarian carcinoma and para-carcinoma tissues

The GEPIA website (<http://gepia.cancer-pku.cn/>) was utilized to analyze the transcriptome data of ovarian carcinoma ($n=426$) and the paired normal tissues ($n=88$) in humans, and the DEGs were identified as a P -value < 0.05 and $\log_2FC > 1$ between ovarian carcinoma and para-carcinoma tissues.

Cell culture

All the ovarian cancer cell lines (SKOV3 and HO-8910) were cultured with RPMI 1640 medium (R5886, Sigma-Aldrich, UK) supplemented with 10% fetal calf serum (F0193, Sigma-Aldrich, UK) and incubated at 37 °C and 5% CO₂. The THP-1 monocytes (human leukemia monocytic cell line) were treated with PMA (100 ng/ml; P8139, Sigma-Aldrich) for 48 h to differentiate into macrophages.

For the preparation of the conditional medium from the macrophages, macrophages derived from THP-1 cells were treated with recombinant human CXCL10 (200 ng/mL; HY-P7226, MedChemExpress, USA) dissolved in ddH₂O at a stock concentration of 200 µg/mL, or with ddH₂O (control) for 24 h. Following this treatment, the CXCL10-containing medium was discarded, and the macrophages were incubated with fresh culture medium for an additional 48 h. The medium collected after this 48-h period was used as the conditioned medium for treating ovarian cancer cells.

Cell counting Kit-8 (CCK-8)

For the cellular proliferation assays, ovarian cancer cells were plated in a 96-well plate (2 × 10³ cells/well) and treated with or without the addition of CXCL10 (200 ng/mL) or the CM from the CXCL10-treated macrophages, as described previously. After 24 h and 48 h, the cells were incubated with the CCK-8 solution (C0005, TargetMol, USA) for 2 h. The absorbance values were measured by a multifunctional microplate reader (Cytation 5, BioTek, USA) at a wavelength of 450 nm. All of the experiments were repeated at least 3 times.

Transwell invasion assay

The cell invasion assay was performed with a transwell chamber (3422, Corning, USA). Matrigel (C0372, Beyotime, China) was diluted in serum-free medium at a 1:6 ratio, then applied to the upper surface of the transwell and incubated at 37 °C for 2 h, following the manufacturer's instructions. After the matrigel had set, the transwells were placed into the 24-well plate with 200 µL of the cell suspension (5 × 10⁴ cells) on top of the matrigel layer. We added CXCL10 (200 ng/mL) or CM (from CXCL10-treated macrophages) to the 24-well plate, which is in the underside of the transwell. After 12 h of incubation at 37 °C with 5% CO₂, the cells in transwells were fixed with 4% paraformaldehyde fix solution (P0099, Beyotime), stained with crystal violet staining solution (C0121, Beyotime) and removed the matrigel in the interior part of the transwell before visualization. At least three replications were conducted.

Wound-healing assay

The ovarian cancer cells were seeded in a 24-well plate (5 × 10⁴ cells per well) for 12 h and mechanically wounded. The serum-free medium containing CXCL10 (200 ng/mL), or CM from macrophages treated with or without CXCL10 was added into the wells. The images of the wounded areas were captured under the light microscope at 0 h and 10 h after the treatment. The area of the wound was quantified with Image J software (<http://rsb.info.nih.gov>). At least three replications were conducted.

Apoptosis assay

The cells were treated with CXCL10 (direct) or CM from THP-1 (indirect) for 24 h. The apoptotic cells were detected with the Annexin V-FITC apoptosis detection kit (C1062L, Beyotime), following the manufacturer's instructions. A CytoFLEX Flow Cytometer (Beckman Coulter, USA) was used to examine the apoptotic rate of cells in each group.

Colony-formation assay

The SKOV3 cells were seeded in a 6-well plate (1 × 10³ cells per well), and were treated with CXCL10 (200 ng/mL) for 48 h. The culture medium containing 200 ng/mL of CXCL10 was replaced every two days. After 12 days, the cells were washed with PBS and stained with the crystal violet staining solution (C0121, Beyotime) for visualization under the light microscope.

Western blot

The SKOV3 cells treated with CXCL10 (200 ng/mL) were harvested and lysed in the RIPA lysis buffer (P1045, Beyotime) containing protease inhibitors and phosphatase inhibitors (C0001 and C0004, TargetMol, USA). The processes of protein extraction and western blot were consistent with our previous protocol [35]. The following primary antibodies and dilutions were used: FAK (1:1000; 1700-1, Epitomics, USA), phosphotyrosine (Y) 397-FAK (1:1000; 3283S, Cell Signaling Technology, USA), phospho-Y576/577-FAK (1:1000; ab76244, Abcam, UK), and GAPDH (1:1000; ab9485, Abcam). The secondary antibodies were horseradish peroxidase-conjugated anti-rabbit or anti-mouse IgG (1:5000; Jackson, USA). The chemiluminescent signal for each target protein was quantified by Image J software (<http://rsb.info.nih.gov>). Phosphorylated protein levels were normalized to their respective total protein levels, and total protein intensities were normalized to GAPDH. All the raw gel figures are supplied as the supplementary materials.

RNA sequencing and pathway enrichment analysis

The macrophages derived from THP-1 cells were treated with CXCL10 (200 ng/mL) or control solution (ddH₂O) for 24 h, as mentioned previously. Then the total RNA was isolated with RNAiso Plus reagent (9108; Takara, Japan) according to the manufacturer's instructions. After RNA purity and integrity were assessed, 2 µg of total RNA per sample were reverse transcribed for cDNA library construction. The cDNA fragments were sequenced on an Illumina HiSeq platform (Illumina). TPM (transcripts per kilobase million) was used to compare the expression of genes between CXCL10-treated macrophages and the control macrophages. A gene was considered a DEG when it met the following criteria: a twofold cut-off change (\log_2 -fold change > 1) in transcript levels and q (adjusted p) value < 0.05. GO analysis and KEGG datasets were used to calculate the significance of the enrichment of DEGs in each pathway. The RNA sequencing data were deposited in the NCBI's Gene Expression Omnibus database (GSE253899).

Statistical analysis

All data were analyzed using the R software (version 4.2.1). The unpaired Student's t -test (T.test in R) was used to compare the differences between two groups. All data are shown as the mean \pm standard deviation (SD). Statistically significant differences were considered at a P value < 0.05.

Results

Dysregulated immune chemokines are present in both obesity and ovarian carcinoma

To investigate the potential relationship between obesity and ovarian carcinoma, we analyzed the differentially expressed genes (DEGs) ($P < 0.05$ and $\log_2FC > 1$) in adipose tissues associated with obesity and in ovarian carcinoma, respectively. First, RNA-seq datasets of subcutaneous adipose tissue from metabolically-healthy lean (MHL) individuals were compared with those of metabolically-unhealthy obese (MUO) and metabolically-healthy obese (MHO) individuals, respectively, to obtain the DEGs of adipose tissues. Additionally, DEGs of the long non-coding RNAs (lncRNAs) profiling of the adipose tissues were identified from the dataset GSE110729. Finally, we intersected the DEGs associated with obesity (from GSE152991 and GSE110729) with those associated with ovarian carcinoma (from TCGA database), identifying 127 positively correlated genes (Fig. 1A). And GO enrichment shows these 127 genes are related to immune cell activation and immune responses (Fig. 1B), suggesting that immunity and immune activation play roles in the interaction between adipose tissue and ovarian carcinoma.

Given the complex factors associated with progressive obesity, we further analyzed the datasets of the adipose tissues from mice fed with a high-fat diet (HFD) or standard-chow diet (SCD) for 8 weeks (GSE132885). By intersecting these datasets, we identified 24 overlapping DEGs (Fig. 1C). Among these, the chemokines CXCL10 and CCL3, which are involved in inflammation, stand out as potential key linkages between obesity and ovarian carcinoma (Fig. 1D). These findings suggest that inflammation induced by adipose tissue in obesity may play a crucial role in the development of ovarian carcinoma.

The enhanced CXCL10 in white adipocyte of mouse HFD model

To determine the origin of chemokines in adipose tissue, we further analyzed the expression of CXCL10 and CCL3 in white adipose tissues from the peri-ovarian fat pad and inguinal fat pad of HFD and SCD mice, based on single-cell RNA sequencing datasets. For the peri-ovarian fat pad, we clustered all cells into eight cell types: smooth muscle cells (SMC), NK and T cells (T_NK), B cells (B), myeloid cells (Mye), endothelial cells (Endo), adipocytes (APC), adipose stem and progenitor cells (ASPC), and mesothelial cells (Mesothelial; Fig. 2A-B). CXCL10 was specifically expressed in APCs, while CCL3 showed minimal expression across all cell types (Fig. S1A). Additionally, the expression of CXCL10 was significantly higher in the adipocytes of HFD mice compared to those of SCD mice ($P < 0.05$; Fig. 2C), which is consistent with the enhanced expression of CXCL10 in the adipose tissue of obese mice.

We also analyzed the datasets from the inguinal fat pads of HFD and SCD mice (GSE176171). 37,994 single-cell transcriptome data in total were obtained and classified into 10 cell clusters [mesothelial cell (Mesothelial), adipose stem and progenitor cell (ASPC), adipocytes (APC), endometrial cell (Endometrial), epithelial cell (Epi), endothelial cell (Endo), myeloid cell (Mye), B cell, T cells, and smooth muscle cell (SMC)] with the specific cell markers (Fig. 2D-E). Consistent with the results from the peri-ovarian fat pad, CCL3 showed very low expression, but CXCL10 showed specifically abundant expression in APCs (Fig. S1B). In addition, the expression levels of CXCL10 were also increased in APCs from HFD mice compared to those from SCD mice ($P < 0.05$; Fig. 2F). These results indicate that CXCL10 expression in APCs is increased under the status of obesity.

CXCL10 accelerates the migration in ovarian cancer cells

The expression of CXCL10 and its receptor, CXCR3, was significantly elevated in ovarian cancer, as shown by data from the GEPIA database, indicating a correlation between CXCL10 and ovarian cancer (Fig. 3A). To

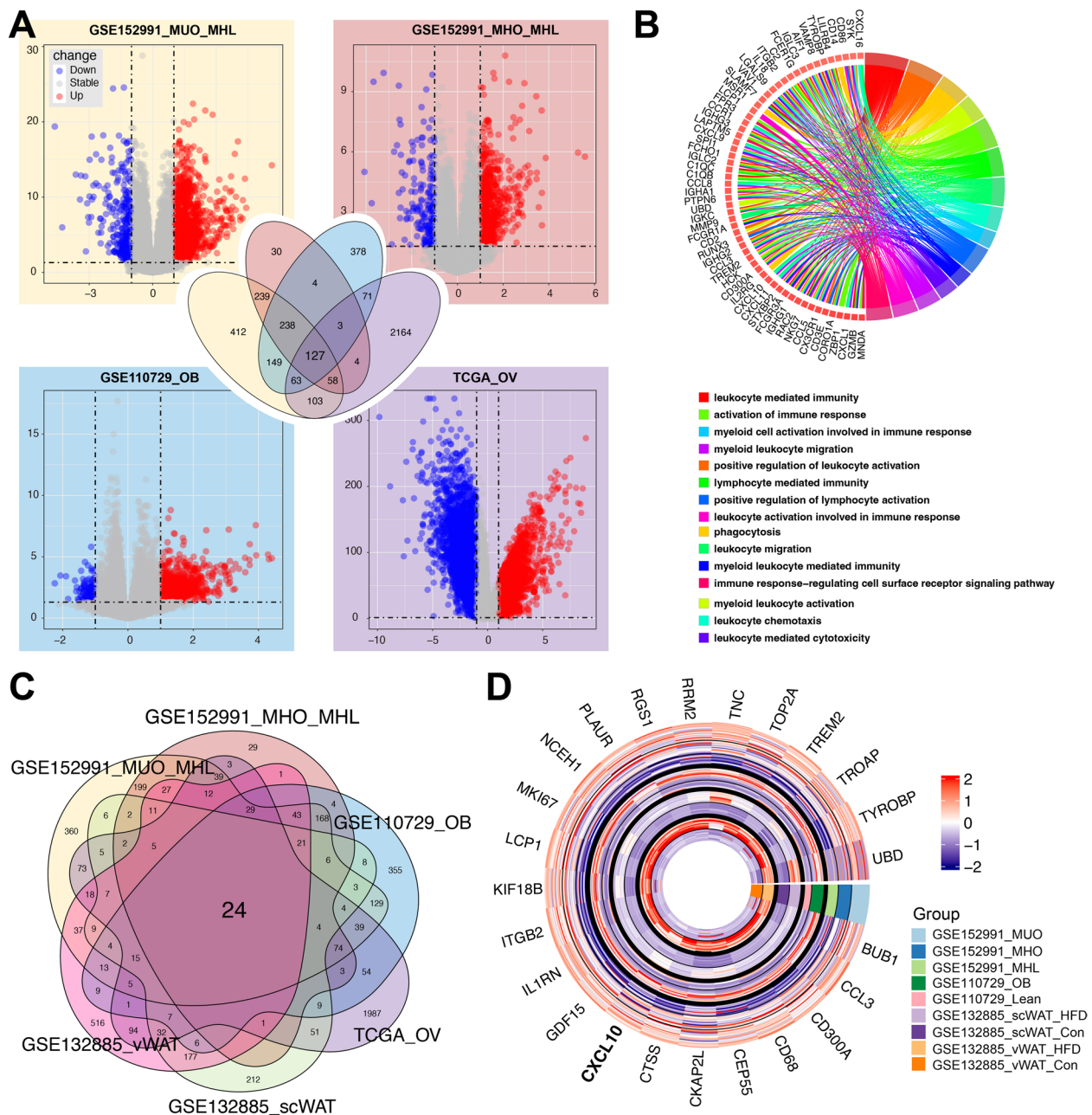


Fig. 1 The dysregulated genes in both obese adipose tissues from humans and mice and ovarian carcinoma. **A** The volcano plot showed differentially expressed genes (P -value < 0.05 and $\log_{2}FC > 1$) in obese or ovarian carcinoma compared to their controls. GSE152991_MUO_MHL showed the differentially expressed genes in white adipose tissue between metabolically unhealthy obese (MUO) and metabolically healthy lean (MHL). GSE152991_MHO_MHL showed the differentially expressed genes in white adipose tissue between metabolically healthy obese (MHO) and metabolically healthy lean (MHL). GSE110729_OB indicated differentially expressed genes in samples with a BMI of 47–68 compared to those with a BMI of 20–23. TCGA_OV indicated differentially expressed genes in ovarian carcinoma compared to normal samples. The Venn plots indicated the shared up-regulated genes in both obese and ovarian carcinomas in humans. **B** The GO plot shows the GO enrichment analysis for the 127 shared genes. **C, D** The expression of 24 shared up-regulated genes in both obese and ovarian carcinoma from both humans and mice

confirm the direct effects of CXCL10 on ovarian cancer cells, we conducted cellular assays to evaluate its impact on the proliferation, migration, and invasion of SKOV3 and HO-8910 cells. As shown in Fig. 3B and Fig. S2A,

CXCL10 significantly increased the migration rate of SKOV3 and HO-8910 cells in the wound healing assay. Similarly, CXCL10 treatment markedly enhanced the invasion ability of SKOV3 and HO-8910 cells (Fig. 3C,

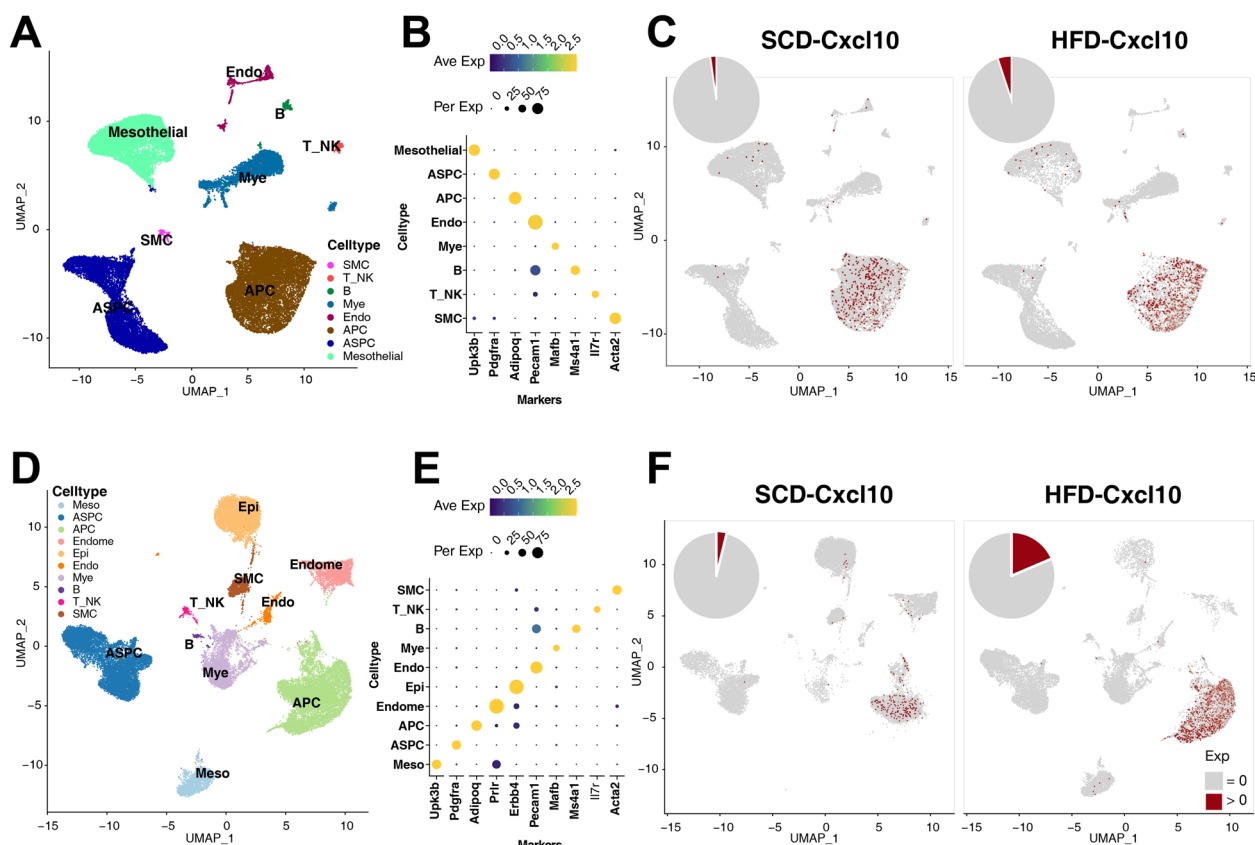


Fig. 2 The expressions of Cxcl10 in white adipose from high-fat diet or standard-chow diet mice. **A** Cell types of mouse peri-ovarian white adipose from single-cell datasets of high-fat diet (HFD) and standard-chow diet (SCD). **B** The specific markers for each cell type of the mouse peri-ovarian white adipose. **C** The expression and the expressed ratio of CXCL10 in peri-ovarian white adipose from HFD and SCD mice. **D** Cell types of mice inguinal white adipose from single-cell datasets of HFD and SCD. **E** The specific markers for each cell type. **F** CXCL10 expression and ratio in inguinal white adipose from HFD and SCD mice

Fig. S2B). However, there was no significant effect on proliferation, apoptosis, or colony formation of SKOV3 cells between the groups with or without CXCL10 (Fig. 3D-3E). For HO8910 cells, CXCL10 partially increased cell viability but had no effect on cell apoptosis (Fig. S2C-2D). These results suggest that CXCL10 may directly promote the migration of ovarian cancer cells without significantly affecting cell proliferation or apoptosis.

CXCL10 increases the phosphorylation of FAK in SKOV3 cells

Given the important roles of FAK signaling in tumor cell adhesion and migration, we further elucidate the possible mechanisms underlying the effect of CXCL10 on the migration of SKOV3 cells. CXCL10 significantly increased protein levels of FAK and phospho-FAK (Tyr576/577) in SKOV3 cells (Fig. 4), but it did not significantly affect the autophosphorylation of FAK at the tyrosine 397 site. These findings suggest that CXCL10 may enhance the migration of ovarian cancer cells by

increasing FAK expression and activating the phosphorylation of FAK.

CXCL10 accelerates migration and invasion of ovarian cancer cells through immune microenvironment

Since CXCL10 is a key chemokine that recruits immune cells to the tumor microenvironment and influences tumor progression, we further investigated its effects by treating SKOV3 and HO-8910 cells with conditioned medium generated from CXCL10-treated macrophages derived from the THP-1 cell. Interestingly, the conditioned medium from CXCL10-treated macrophages significantly increased the migration rate and invasive ability of these two ovarian cells compared to the medium from NC-treated macrophages (Fig. 5A, 5C; Fig. S2E-2F). However, there were no significant differences in proliferation or apoptosis in ovarian cancer cells upon the addition of the conditioned medium (Fig. 5B, 5D-E; Fig. S2G-2H). Beyond its direct effects, CXCL10 may also indirectly

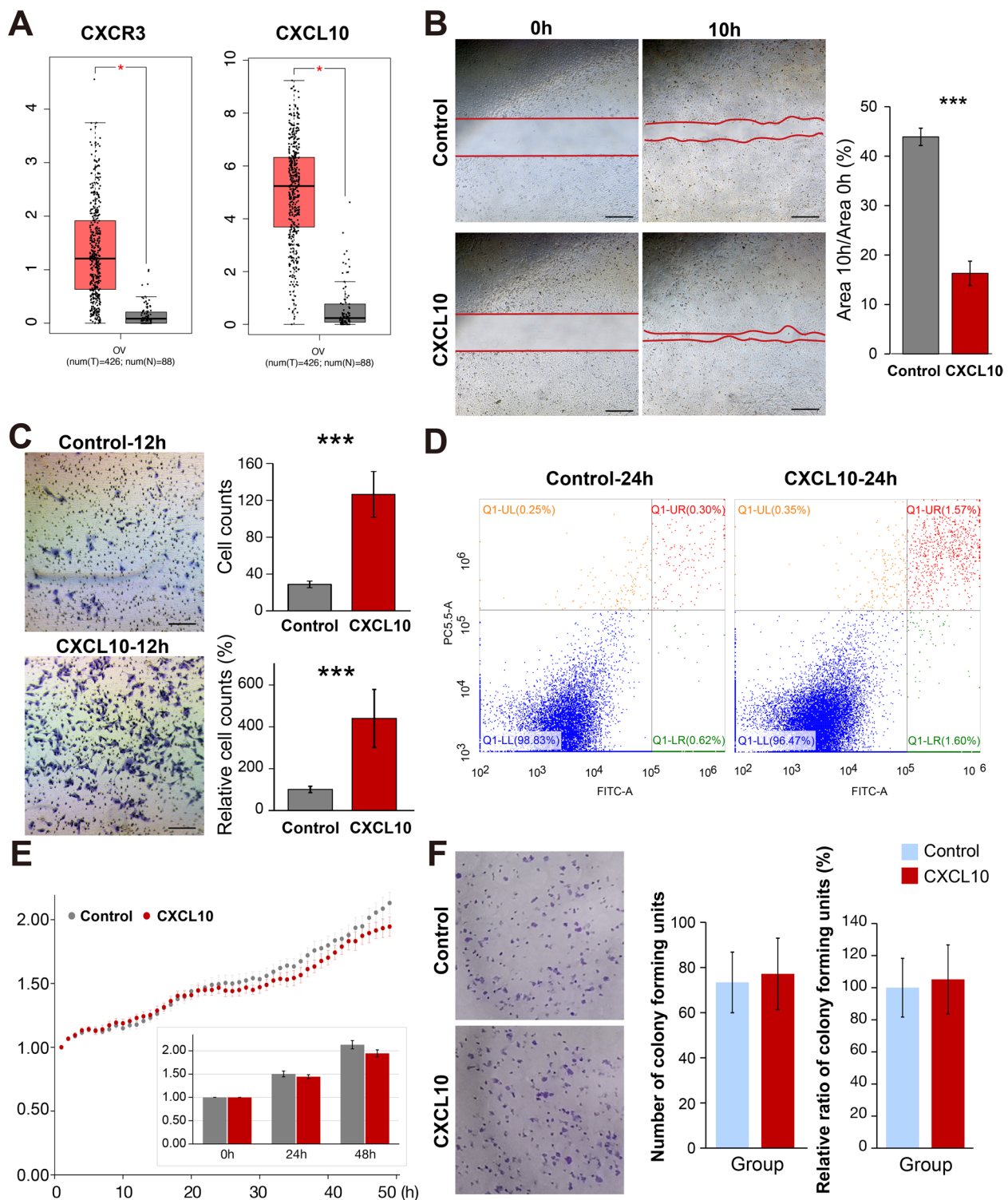


Fig. 3 The effect of CXCL10 on migration, invasion, colony-formation, apoptosis, and proliferation of SKOV3 cells. **A** The expression of CXCR3 and CXCL10 in the ovarian carcinoma from the GEPIA database. **B** The significantly enhanced of migration in the SKOV3 cell line with the addition of CXCL10 ($P < 0.001$). **C** The significantly enhanced invasion in the SKOV3 cell line with the addition of CXCL10 ($P < 0.001$). **D** The apoptosis of SKOV3 cells treated with or without CXCL10. **E, F** The proliferation includes CCK8 assay (**E**) and colony-formation assay (**F**) of SKOV3 cells treated with or without CXCL10 ($P > 0.05$). Bar plots show the mean \pm SEM. *** indicates a $P < 0.001$

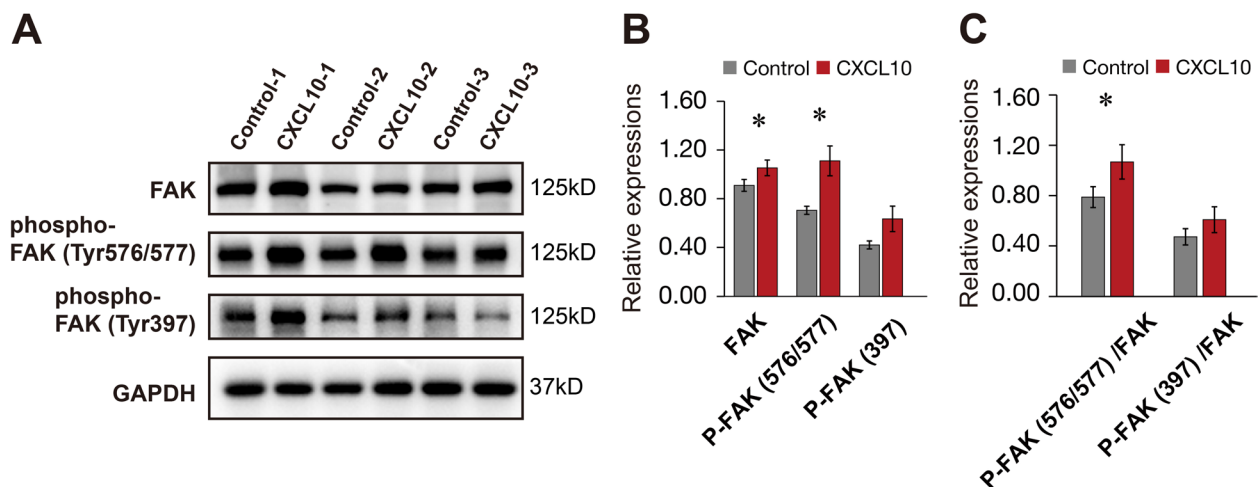


Fig. 4 CXCL10 enhanced the expression and activation of FAK in SKOV3 cell lines. **A** The expression and phosphorylation of FAK in the SKOV3 cells treated with or without CXCL10. **B, C** The quantification of the relative expression of FAK in the western blot. Bar plots show the mean \pm SEM. * indicates a $P < 0.05$

influence the invasion and migration ability of ovarian cancer cells by priming and activating macrophages within the tumor microenvironment.

The increased C1Q+ macrophages induced by CXCL10 may accelerate migration of ovarian cancer cells

To explore the mechanisms by which CXCL10 primes macrophages, we performed RNA sequencing analysis between the macrophages treated with CXCL10 and control. As shown in Fig. 6A, CXCL10 treatment did not significantly differentiate the macrophages to M1 or M2 polarization. However, markers for tumor-associated macrophages (TAM), i.e., C1QA, C1QC, IL4R, and CCL24, were markedly upregulated in CXCL10-treated macrophages compared to controls.

To further confirm the characteristics of these macrophages and their interactions with adipose tissue, we analyzed gene expression patterns in macrophages from the white adipose tissues of HFD and SCD mice. Interestingly, the expression levels of C1qa ($P < 0.05$), C1qb ($P < 0.01$), C1qc ($P < 0.05$), Il4ra ($P < 0.05$), Il4 ($P < 0.05$), and Ccl24 ($P = 0.102$) were all significantly elevated in macrophages from the white adipose tissues of HFD mice (Fig. 6B-H). Combined with our previous finding of abundant CXCL10 expression in APCs (Fig. 2B), these results suggest that elevated CXCL10 levels in APCs may increase the proportion of C1Q+ macrophages and enhance CCL24 production, playing a critical role in regulating the tumor microenvironment and promoting ovarian cancer metastasis.

Discussion

Due to drastic lifestyle changes, particularly the increased consumption of high-fat diets and decreased physical activity, overweight or obesity has become a worldwide epidemic problem for human beings and poses a significant risk to human health [36], including diabetes mellitus, cardiovascular disease, infertility, and even the development of some cancers [37, 38]. Obesity-induced inflammation may increase cancer risk through multiple mechanisms [7, 39], and validating the shared genes that are simultaneously dysregulated in both obesity and tumors is a promising way to reveal the interaction between obesity and cancer. In this study, we first verified 24 common genes that were synchronously up-regulated in both ovarian cancer cells from obese women and adipose tissues from HFD-induced obese mice, based on the public RNA sequencing datasets. Given the potential functions of chemokines in immune and inflammatory response, which play an important role in both obesity and cancer progression, CXCL10 and CCL3 drew our attention. Moreover, we further verified that CXCL10, but not CCL3 was abundantly expressed in the adipocyte at the single-cell level in both the peri-ovarian fat pad and the inguinal fat pad. CXCL10 manifested a significant increase in adipocytes from HFD mice compared to those from SCD mice, leading us to focus on CXCL10 in the following study.

CXCL10 showed opposite effects on the development of tumors mediated by different mechanisms [40–48]. For example, the CXCL10 produced by tumors can recruit CXCR3+ T cells and NK cells to suppress tumors

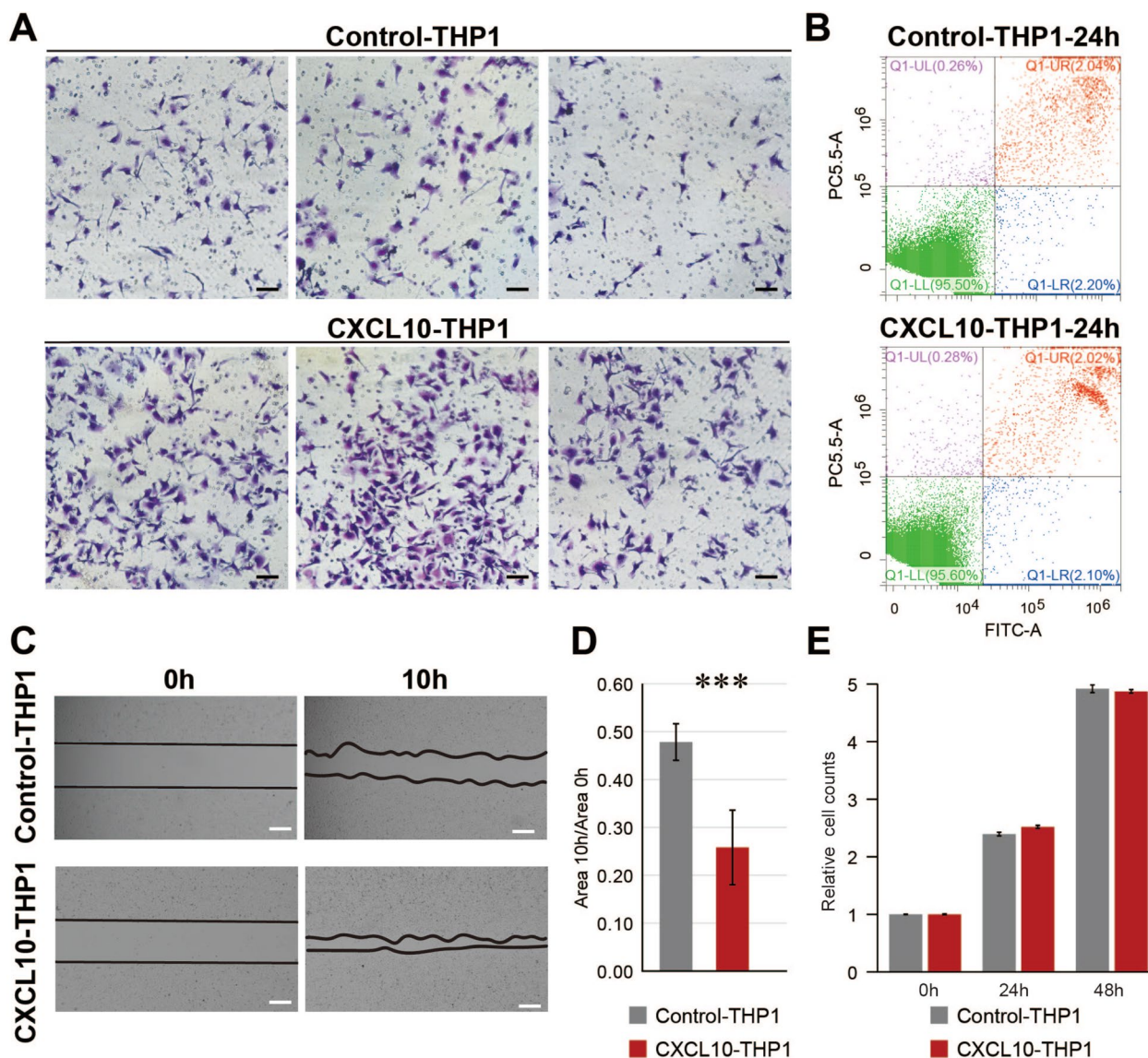


Fig. 5 The effects of conditional medium from CXCL10-treated macrophages on migration, invasion, proliferation, and apoptosis of SKOV3 cells. **A** The conditional medium from CXCL10-treated macrophages (THP-1 cell) enhanced the invasion of SKOV3 cells. **B** The apoptosis of SKOV3 cells treated with the conditional medium from CXCL10-treated macrophages. **C, D** The migration of SKOV3 cells treated with the conditional medium from CXCL10-treated macrophages. **E** The proliferation of SKOV3 cells treated with conditional medium from CXCL10-treated macrophages. *** indicates a $P < 0.001$

[41, 45, 47, 48]. However, CXCL10 can also increase the metastasis of CXCR3+ tumor cells [43, 44, 49–51]. In this study, we found that CXCL10 can increase the expression and phosphorylation of FAK (Y576/577) and improve the migration and invasion of ovarian cancer cells in vitro. As an important regulator of cell migration and angiogenesis [52], FAK plays an important role in the formation and maturation of focal adhesions that are linked to the intracellular actin cytoskeleton [53]. FAK(Y397) is an autophosphorylation site initializing

the activation of FAK signaling and facilitates FAK combination with the actin-linking protein vinculin, which is required for highly dynamic tissue remodeling during development [35, 54, 55]. After the autophosphorylation of FAK (Y397), the FAK phosphorylation at Y576/577 site cause maximal FAK catalytic activation [35, 56, 57]. Our findings reveal that CXCL10 significantly increases phosphorylation at the FAK Y576/577 sites, while exerting no significant effect on phosphorylation at the Y397 site. This suggests that adipose derived CXCL10-driven

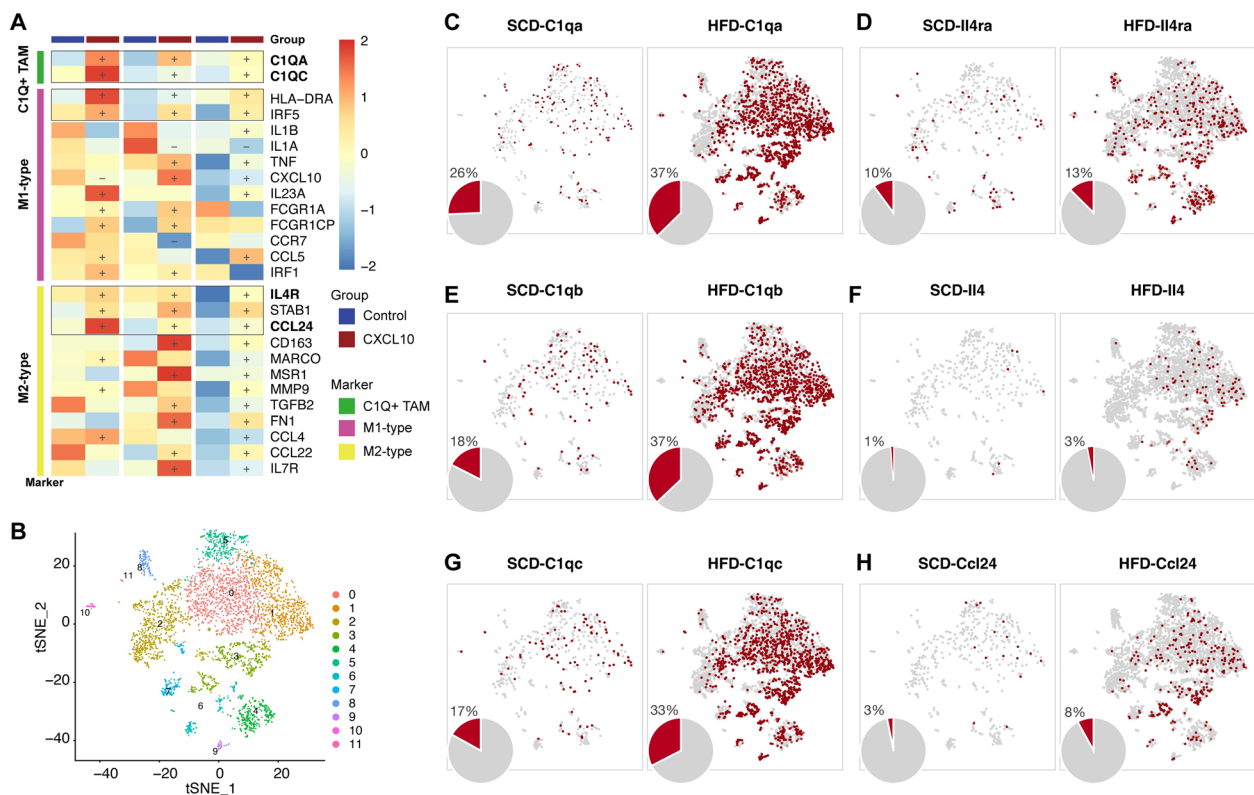


Fig. 6 The increased expression of C1Qs in CXCL10-treated macrophages and macrophages from adipose tissue. **A** The addition of CXCL10 increased the expression of C1QA and C1QC in macrophages. + indicates the up-regulation in CXCL10-added macrophages with the fold change > 1.2; — indicates the down-regulation in CXCL10-added macrophages with the fold change > 1.2. **B** The sub-clusters in macrophages. **C-H** The increased expression ratios of C1qa (P value < 0.05), C1qb (P value < 0.01), C1qc (P value < 0.05), Il4ra (P value < 0.05), Il4 (P value < 0.05), and Ccl24 (P value = 0.102) in macrophages from HFD mice compared to those from SCD mice

catalytic activation of FAK is a key process that contributing to the migration of ovarian cancer. Additionally, other intricate signaling pathways and regulatory mechanisms associated with CXCL10-regulated ovarian cancer cell migration, such as AKT and MAPK, also merit further investigation.

Of interest, we found that the conditional medium from the macrophages treated with CXCL10 also enhanced the migration and invasion of ovarian cancer cell lines. This result suggested that the excess CXCL10 secreted by adipose tissues may transform the state of macrophages, subsequently influencing the metastatic behavior of ovarian cancer cells. Previous studies have shown that macrophages are key immune cells in the tumor microenvironment [58–60], and the direct communication between macrophages and tumor cells can promote the tumor development [59, 61, 62].

The classical inflammatory markers for M1/M2 macrophage polarization manifested no significant changes, while the markers for tumor-associated macrophages, namely C1QA, C1QC, CCL24, and IL4R, were all significantly increased in macrophages treated with CXCL10.

C1Q has been shown to promote the migration and adhesion of various human malignant tumors, thereby facilitating tumor growth and migration through non-classical pathways. Notably, C1Q is present in the ascitic fluid associated with ovarian cancer, rather than within the ovarian cancer cells themselves [63, 64]. And the C1Q+ macrophage is the driver of cancer progression, as reported in previous studies [65]. CCL24 and the IL4/IL4R pathway can facilitate migration and invasion of tumor cells [66, 67]. Similarly, the expression levels of C1qa, C1qb, C1qc, Ccl23, Il4, and Il4ra were significantly elevated in macrophages from the subcutaneous adipose tissue of HFD mice. Thus, the excess CXCL10 secreted by adipose tissues potentially accelerates the migration of ovarian cancer in obese patients by altering the tumor microenvironment, at least partly mediated by modification of tissue resident macrophages. Since the DEGs in C1Q+ macrophages include both transcriptional factors and secreted proteins, further investigation is warranted to determine whether the interactions between C1Q+ macrophages

and ovarian cancer cells are mediated exclusively by secreted factors or also involve direct cell–cell contact.

In conclusion, we propose that high CXCL10 levels secreted by adipocytes of obese individuals could exacerbate migration of ovarian cancer through direct and indirect mechanisms. Directly, CXCL10 enhances the migration and invasion of ovarian cancer cells through activation of FAK signaling. Indirectly, CXCL10 increases the expression of C1QA, C1QC, CCL24, and IL4R in macrophages, leading to their transformation into tumor-associated macrophages (TAMs), which further enhance the migration of ovarian cancer cell. We highlight CXCL10 as a hub between obesity and ovarian cancer, particularly its role in promoting the migration of ovarian cancer cells. However, due to the absence of in vivo verification, the significance of CXCL10 in the immune microenvironment and its impact on ovarian cancer metastasis in vivo warrant further research.

Abbreviations

ASPC	Adipose stem and progenitor cell
APC	Adipocytes
FA	Focal adhesion
FAK	Focal adhesion kinase
HFD	High-fat diet
lncRNA	Long non-coding RNA
MHL	Metabolically-healthy lean
MUO	Metabolically-unhealthy obese
SCD	Standard-chow diet
SMC	Smooth muscle cell
TAM	Tumor-associated macrophage
TPM	Transcripts per kilobase million

Supplementary Information

The online version contains supplementary material available at <https://doi.org/10.1186/s13048-024-01568-0>.

Supplementary Material 1: Figure S1. The expression of Cxcl10 and Ccl3 in white adipose from both HFD and SCD mice.

Supplementary Material 2: Figure S2. The effects of CXCL10 and conditional medium from CXCL10-treated macrophages on migration, invasion, proliferation, and apoptosis of HO-8910 cells. (A–D) The effect of CXCL10 on the migration (A), invasion (B), apoptosis (C), and proliferation (D) of HO-8910 cells. (E–H) The effect of the conditional medium from CXCL10-treated macrophages on the migration (E), invasion (F), apoptosis (G), and proliferation (H) of HO-8910 cells. *: $P < 0.05$; **: $P < 0.01$; ***: $P < 0.001$.

Supplementary Material 3.

Acknowledgements

Not applicable.

Authors' contributions

Conceptualization: ZW, QQ, LG. Methodology: ZW, YL, QQ. Investigation: ZW, QQ, YL, QZ, JF, FH. Supervision: LG. Writing—original draft: ZW, QQ. Writing—review & editing: ZW, QQ, LG. All authors contributed to the article and approved the submitted version.

Funding

This research was funded by the Shanghai Sailing Program (23YF1457700), National Natural Science Foundation of China (82120108011 & 82371699), National Key Research and Development Project (2022YFC2704602 &

2022YFC2704502), and the Shanghai Municipal Health Commission (20234Y0113).

Data availability

The RNA sequencing data were deposited in the NCBI's Gene Expression Omnibus database (GSE253899).

Declarations

Ethics approval and consent to participate

Not applicable.

Consent for publication

Not applicable.

Competing interests

The authors declare no competing interests.

Received: 9 July 2024 Accepted: 28 November 2024

Published online: 19 December 2024

References

- Karczewski J, Sledzinska E, Batur A, Jonczyk I, Maleszko A, Samborski P, et al. Obesity and inflammation. *Eur Cytokine Netw*. 2018;29(3):83–94. <https://doi.org/10.1684/ecn.2018.0415>.
- Wang T, He C. Pro-inflammatory cytokines: The link between obesity and osteoarthritis. *Cytokine Growth Factor Rev*. 2018;44:38–50. <https://doi.org/10.1016/j.cytogfr.2018.10.002>.
- Kochumon S, Madhoun AA, Al-Rashed F, Azim R, Al-Ozairi E, Al-Mulla F, et al. Adipose tissue gene expression of CXCL10 and CXCL11 modulates inflammatory markers in obesity: implications for metabolic inflammation and insulin resistance. *Ther Adv Endocrinol Metab*. 2020;11:2042018820930902. <https://doi.org/10.1177/2042018820930902>.
- Nunemaker CS, Chung HG, Verrilli GM, Corbin KL, Upadhye A, Sharma PR. Increased serum CXCL1 and CXCL5 are linked to obesity, hyperglycemia, and impaired islet function. *J Endocrinol*. 2014;222(2):267–76. <https://doi.org/10.1530/JOE-14-0126>.
- Anderson EK, Gutierrez DA, Hasty AH. Adipose tissue recruitment of leukocytes. *Curr Opin Lipidol*. 2010;21(3):172–7. <https://doi.org/10.1097/MOL.0b013e3283393867>.
- Surmi BK, Hasty AH. The role of chemokines in recruitment of immune cells to the artery wall and adipose tissue. *Vascul Pharmacol*. 2010;52(1–2):27–36. <https://doi.org/10.1016/j.vph.2009.12.004>.
- Kolb R, Sutterwala FS, Zhang W. Obesity and cancer: inflammation bridges the two. *Curr Opin Pharmacol*. 2016;29:77–89. <https://doi.org/10.1016/j.coph.2016.07.005>.
- Rosen ED, Spiegelman BM. Adipocytes as regulators of energy balance and glucose homeostasis. *Nature*. 2006;444(7121):847–53. <https://doi.org/10.1038/nature05483>.
- Calle EE, Kaaks R. Overweight, obesity and cancer: epidemiological evidence and proposed mechanisms. *Nat Rev Cancer*. 2004;4(8):579–91. <https://doi.org/10.1038/nrc1408>.
- Foong KW, Bolton H. Obesity and ovarian cancer risk: A systematic review. *Post Reprod Health*. 2017;23(4):183–98. <https://doi.org/10.1177/2053369117709225>.
- Bader JE, Wolf MM, Lupica-Tondo GL, Madden MZ, Reinfeld BI, Arner EN, et al. Obesity induces PD-1 on macrophages to suppress anti-tumour immunity. *Nature*. 2024;630(8018):968–75. <https://doi.org/10.1038/s41586-024-07529-3>.
- Islami F, Goding Sauer A, Gapstur SM, Jemal A. Proportion of Cancer Cases Attributable to Excess Body Weight by US State, 2011–2015. *JAMA Oncol*. 2019;5(3):384–92. <https://doi.org/10.1001/jamaoncol.2018.5639>.
- Mei S, Chen X, Wang K, Chen Y. Tumor microenvironment in ovarian cancer peritoneal metastasis. *Cancer Cell Int*. 2023;23(1):11. <https://doi.org/10.1186/s12935-023-02854-5>.

14. Naora H, Montell DJ. Ovarian cancer metastasis: integrating insights from disparate model organisms. *Nat Rev Cancer*. 2005;5(5):355–66. <https://doi.org/10.1038/nrc1611>.
15. Lotan T, Hickson J, Souris J, Huo D, Taylor J, Li T, et al. c-Jun NH2-terminal kinase activating kinase 1/mitogen-activated protein kinase kinase 4-mediated inhibition of SKOV3ip.1 ovarian cancer metastasis involves growth arrest and p21 up-regulation. *Cancer Res*. 2008;68(7):2166–75. <https://doi.org/10.1158/0008-5472.CAN-07-1568>.
16. Kenny HA, Krausz T, Yamada SD, Lengyel E. Use of a novel 3D culture model to elucidate the role of mesothelial cells, fibroblasts and extracellular matrices on adhesion and invasion of ovarian cancer cells to the omentum. *Int J Cancer*. 2007;121(7):1463–72. <https://doi.org/10.1002/ijc.22874>.
17. Zlotnik A, Yoshie O. The chemokine superfamily revisited. *Immunity*. 2012;36(5):705–16. <https://doi.org/10.1016/j.immuni.2012.05.008>.
18. O'Hayre M, Salanga CL, Handel TM, Allen SJ. Chemokines and cancer: migration, intracellular signalling and intercellular communication in the microenvironment. *Biochem J*. 2008;409(3):635–49. <https://doi.org/10.1042/BJ20071493>.
19. Lupi LA, Delella FK, Cuciolo MS, Romagnoli GG, Kaneno R, Nunes IDS, et al. P-MAPA and Interleukin-12 Reduce Cell Migration/Invasion and Attenuate the Toll-Like Receptor-Mediated Inflammatory Response in Ovarian Cancer SKOV-3 Cells: A Preliminary Study. *Molecules*. 2019;25(1). <https://doi.org/10.3390/molecules25010005>.
20. Silveira HS, Lupi LA, Romagnoli GG, Kaneno R, da Silva NI, Favaro WJ, et al. P-MAPA activates TLR2 and TLR4 signaling while its combination with IL-12 stimulates CD4+ and CD8+ effector T cells in ovarian cancer. *Life Sci*. 2020;254:117786. <https://doi.org/10.1016/j.lfs.2020.117786>.
21. Jones VS, Huang RY, Chen LP, Chen ZS, Fu L, Huang RP. Cytokines in cancer drug resistance: Cues to new therapeutic strategies. *Biochim Biophys Acta*. 2016;1865(2):255–65. <https://doi.org/10.1016/j.bbcan.2016.03.005>.
22. Vilgelm AE, Richmond A. Chemokines Modulate Immune Surveillance in Tumorigenesis, Metastasis, and Response to Immunotherapy. *Front Immunol*. 2019;10:333. <https://doi.org/10.3389/fimmu.2019.00333>.
23. You Y, Li Y, Li M, Lei M, Wu M, Qu Y, et al. Ovarian cancer stem cells promote tumour immune privilege and invasion via CCL5 and regulatory T cells. *Clin Exp Immunol*. 2018;191(1):60–73. <https://doi.org/10.1111/cei.13044>.
24. Moin ASM, Cory M, Choi J, Ong A, Dhawan S, Dry SM, et al. Increased Chromogranin A-Positive Hormone-Negative Cells in Chronic Pancreatitis. *J Clin Endocrinol Metab*. 2018;103(6):2126–35. <https://doi.org/10.1210/jc.2017-01562>.
25. Delitto D, Perez C, Han S, Gonzalo DH, Pham K, Knowlton AE, et al. Downstream mediators of the intratumoral interferon response suppress antitumor immunity, induce gemcitabine resistance and associate with poor survival in human pancreatic cancer. *Cancer Immunol Immunother*. 2015;64(12):1553–63. <https://doi.org/10.1007/s00262-015-1760-y>.
26. Kwaifa IK, Bahari H, Yong YK, Noor SM. Endothelial Dysfunction in Obesity-Induced Inflammation: Molecular Mechanisms and Clinical Implications. *Biomolecules*. 2020;10(2). <https://doi.org/10.3390/biom10020291>.
27. Nagle CM, Dixon SC, Jensen A, Kjaer SK, Modugno F, deFazio A, et al. Obesity and survival among women with ovarian cancer: results from the Ovarian Cancer Association Consortium. *Br J Cancer*. 2015;113(5):817–26. <https://doi.org/10.1038/bjc.2015.245>.
28. Reeves GK, Pirie K, Beral V, Green J, Spencer E, Bull D, et al. Cancer incidence and mortality in relation to body mass index in the Million Women Study: cohort study. *BMJ*. 2007;335(7630):1134. <https://doi.org/10.1136/bmj.39367.495995.AE>.
29. Diaz ES, Karlan BY, Li AJ. Obesity-associated adipokines correlate with survival in epithelial ovarian cancer. *Gynecol Oncol*. 2013;129(2):353–7. <https://doi.org/10.1016/j.ygyno.2013.02.006>.
30. Cifarelli V, Beeman SC, Smith GJ, Yoshino J, Morozov D, Beals JW, et al. Decreased adipose tissue oxygenation associates with insulin resistance in individuals with obesity. *J Clin Invest*. 2020;130(12):6688–99. <https://doi.org/10.1172/JCI141828>.
31. Caputo T, Tran VDT, Bararpour N, Winkler C, Aguilera G, Trang KB, et al. Anti-adipogenic signals at the onset of obesity-related inflammation in white adipose tissue. *Cell Mol Life Sci*. 2021;78(1):227–47. <https://doi.org/10.1007/s00018-020-03485-z>.
32. Love MI, Huber W, Anders S. Moderated estimation of fold change and dispersion for RNA-seq data with DESeq2. *Genome Biol*. 2014;15(12):550. <https://doi.org/10.1186/s13059-014-0550-8>.
33. Satija R, Farrell JA, Gennert D, Schier AF, Regev A. Spatial reconstruction of single-cell gene expression data. *Nat Biotechnol*. 2015;33(5):495–502. <https://doi.org/10.1038/nbt.3192>.
34. Emont MP, Jacobs C, Essene AL, Pant D, Tenen D, Colleluori G, et al. A single-cell atlas of human and mouse white adipose tissue. *Nature*. 2022;603(7903):926–33. <https://doi.org/10.1038/s41586-022-04518-2>.
35. Chen HY, Gao LT, Yuan JQ, Zhang YJ, Liu P, Wang G, et al. Decrease in SHP-1 enhances myometrium remodeling via FAK activation leading to labor. *Am J Physiol Endocrinol Metab*. 2020;318(6):E930–42. <https://doi.org/10.1152/ajpendo.00068.2020>.
36. Blüher M. Obesity: global epidemiology and pathogenesis. *Nat Rev Endocrinol*. 2019;15(5):288–98. <https://doi.org/10.1038/s41574-019-0176-8>.
37. Pati S, Irfan W, Jameel A, Ahmed S, Shahid RK. Obesity and Cancer: A Current Overview of Epidemiology, Pathogenesis, Outcomes, and Management. *Cancers (Basel)*. 2023;15(2). <https://doi.org/10.3390/cancers15020485>.
38. Jiang Y, Gao X, Liu Y, Yan X, Shi H, Zhao R, et al. Cellular atlases of ovarian microenvironment alterations by diet and genetically-induced obesity. *Sci China Life Sci*. 2024;67(1):51–66. <https://doi.org/10.1007/s11427-023-2360-3>.
39. Deng T, Lyon CJ, Bergin S, Caligiuri MA, Hsueh WA. Obesity, Inflammation, and Cancer. *Annu Rev Pathol*. 2016;11:421–49. <https://doi.org/10.1146/annurev-pathol-012615-044359>.
40. Wenzel J, Bekisch B, Uerlich M, Haller O, Bieber T, Tuting T. Type I interferon-associated recruitment of cytotoxic lymphocytes: a common mechanism in regressive melanocytic lesions. *Am J Clin Pathol*. 2005;124(1):37–48. <https://doi.org/10.1309/4EJ9KL7CGDENVLE>.
41. Fujita M, Zhu X, Ueda R, Sasaki K, Kohanbash G, Kastnerhuber ER, et al. Effective immunotherapy against murine gliomas using type 1 polarizing dendritic cells—significant roles of CXCL10. *Cancer Res*. 2009;69(4):1587–95. <https://doi.org/10.1158/0008-5472.CAN-08-2915>.
42. Antonicelli F, Lorin J, Kurdykowski S, Gangloff SC, Le Naour R, Sallenave JM, et al. CXCL10 reduces melanoma proliferation and invasiveness in vitro and in vivo. *Br J Dermatol*. 2011;164(4):720–8. <https://doi.org/10.1111/j.1365-2133.2010.10176.x>.
43. Kawada K, Hosogi H, Sonoshita M, Sakashita H, Manabe T, Shimahara Y, et al. Chemokine receptor CXCR3 promotes colon cancer metastasis to lymph nodes. *Oncogene*. 2007;26(32):4679–88. <https://doi.org/10.1038/sj.onc.1210267>.
44. Kawada K, Sonoshita M, Sakashita H, Takabayashi A, Yamaoka Y, Manabe T, et al. Pivotal role of CXCR3 in melanoma cell metastasis to lymph nodes. *Cancer Res*. 2004;64(11):4010–7. <https://doi.org/10.1158/0008-5472.CAN-03-1757>.
45. Harlin H, Meng Y, Peterson AC, Zha Y, Tretiakova M, Slingluff C, et al. Chemokine expression in melanoma metastases associated with CD8+ T-cell recruitment. *Cancer Res*. 2009;69(7):3077–85. <https://doi.org/10.1158/0008-5472.CAN-08-2281>.
46. Wightman SC, Uppal A, Pitroda SP, Ganai S, Burnette B, Stack M, et al. Oncogenic CXCL10 signalling drives metastasis development and poor clinical outcome. *Br J Cancer*. 2015;113(2):327–35. <https://doi.org/10.1038/bjc.2015.193>.
47. Dengel LT, Norrod AG, Gregory BL, Clancy-Thompson E, Burdick MD, Strieter RM, et al. Interferons induce CXCR3-cognate chemokine production by human metastatic melanoma. *J Immunother*. 2010;33(9):965–74. <https://doi.org/10.1097/CJI.0b013e3181fb045d>.
48. Wennerberg E, Kremer V, Childs R, Lundqvist A. CXCL10-induced migration of adoptively transferred human natural killer cells toward solid tumors causes regression of tumor growth in vivo. *Cancer Immunol Immunother*. 2015;64(2):225–35. <https://doi.org/10.1007/s00262-014-1629-5>.
49. Walser TC, Rifat S, Ma X, Kundu N, Ward C, Goloubeva O, et al. Antagonism of CXCR3 inhibits lung metastasis in a murine model of metastatic breast cancer. *Cancer Res*. 2006;66(15):7701–7. <https://doi.org/10.1158/0008-5472.CAN-06-0709>.
50. Ma X, Norsworthy K, Kundu N, Rodgers WH, Gimotty PA, Goloubeva O, et al. CXCR3 expression is associated with poor survival in breast cancer and promotes metastasis in a murine model. *Mol Cancer Ther*. 2009;8(3):490–8. <https://doi.org/10.1158/1535-7163.MCT-08-0485>.

51. Cambien B, Karimjee BF, Richard-Fiardo P, Bziouech H, Barthel R, Millet MA, et al. Organ-specific inhibition of metastatic colon carcinoma by CXCR3 antagonism. *Br J Cancer*. 2009;100(11):1755–64. <https://doi.org/10.1038/sj.bjc.6605078>.
52. Zhao X, Guan JL. Focal adhesion kinase and its signaling pathways in cell migration and angiogenesis. *Adv Drug Deliv Rev*. 2011;63(8):610–5. <https://doi.org/10.1016/j.addr.2010.11.001>.
53. Pasapera AM, Schneider IC, Rericha E, Schlaepfer DD, Waterman CM. Myosin II activity regulates vinculin recruitment to focal adhesions through FAK-mediated paxillin phosphorylation. *J Cell Biol*. 2010;188(6):877–90. <https://doi.org/10.1083/jcb.200906012>.
54. Heim JB, McDonald CA, Wyles SP, Somnidi-Damodaran S, Squirewell EJ, Li M, et al. FAK auto-phosphorylation site tyrosine 397 is required for development but dispensable for normal skin homeostasis. *PLoS ONE*. 2018;13(7):e0200558. <https://doi.org/10.1371/journal.pone.0200558>.
55. Hu S, Wang Z, Jin C, Chen Q, Fang Y, Jin J, et al. Human amniotic epithelial cell-derived extracellular vesicles provide an extracellular matrix-based microenvironment for corneal injury repair. *J Tissue Eng*. 2022;13:20417314221122124. <https://doi.org/10.1177/20417314221122123>.
56. Lim ST, Mikolon D, Stupack DG, Schlaepfer DD. FERM control of FAK function: implications for cancer therapy. *Cell Cycle*. 2008;7(15):2306–14. <https://doi.org/10.4161/cc.6367>.
57. Tan X, Yan Y, Song B, Zhu S, Mei Q, Wu K. Focal adhesion kinase: from biological functions to therapeutic strategies. *Exp Hematol Oncol*. 2023;12(1):83. <https://doi.org/10.1186/s40164-023-00446-7>.
58. Vitale I, Manic G, Coussens LM, Kroemer G, Galluzzi L. Macrophages and Metabolism in the Tumor Microenvironment. *Cell Metab*. 2019;30(1):36–50. <https://doi.org/10.1016/j.cmet.2019.06.001>.
59. Bied M, Ho WW, Ginhoux F, Bleriot C. Roles of macrophages in tumor development: a spatiotemporal perspective. *Cell Mol Immunol*. 2023;20(9):983–92. <https://doi.org/10.1038/s41423-023-01061-6>.
60. Sadhukhan P, Seiwert TY. The role of macrophages in the tumor microenvironment and tumor metabolism. *Semin Immunopathol*. 2023;45(2):187–201. <https://doi.org/10.1007/s00281-023-00988-2>.
61. Condeelis J, Pollard JW. Macrophages: obligate partners for tumor cell migration, invasion, and metastasis. *Cell*. 2006;124(2):263–6. <https://doi.org/10.1016/j.cell.2006.01.007>.
62. Ji S, Shi Y, Yin B. Macrophage barrier in the tumor microenvironment and potential clinical applications. *Cell Commun Signal*. 2024;22(1):74. <https://doi.org/10.1186/s12964-023-01424-6>.
63. Bulla R, Tripodo C, Rami D, Ling GS, Agostinis C, Guarnotta C, et al. C1q acts in the tumour microenvironment as a cancer-promoting factor independently of complement activation. *Nat Commun*. 2016;7:10346. <https://doi.org/10.1038/ncomms10346>.
64. Kaur A, Sultan SH, Murugaiah V, Pathan AA, Alhamlan FS, Karteris E, et al. Human C1q Induces Apoptosis in an Ovarian Cancer Cell Line via Tumor Necrosis Factor Pathway. *Front Immunol*. 2016;7:599. <https://doi.org/10.3389/fimmu.2016.00599>.
65. Revel M, Sautes-Fridman C, Fridman WH, Roumenina LT. C1q+ macrophages: passengers or drivers of cancer progression. *Trends Cancer*. 2022;8(7):517–26. <https://doi.org/10.1016/j.trecan.2022.02.006>.
66. Lim SJ. CCL24 Signaling in the Tumor Microenvironment. *Adv Exp Med Biol*. 2021;1302:91–8. https://doi.org/10.1007/978-3-030-62658-7_7.
67. Bankaitis KV, Fingleton B. Targeting IL4/IL4R for the treatment of epithelial cancer metastasis. *Clin Exp Metastasis*. 2015;32(8):847–56. <https://doi.org/10.1007/s10585-015-9747-9>.

Publisher's Note

Springer Nature remains neutral with regard to jurisdictional claims in published maps and institutional affiliations.